Title	Selective interaction of Hpn-like protein with nickel, zinc and bismuth in vitro and in cells by FRET
Author(s)	Chang, YY; Lai, YT; Cheng, T; Wang, H; Yang, Y; Sun, H
Citation	Journal of Inorganic Biochemistry, 2015, v. 142, p. 8-14
Issued Date	2015
URL	http://hdl.handle.net/10722/215150
Rights	

Selective interaction of Hpn-like protein with nickel, zinc and bismuth *in vitro* and in cells by FRET

Yuen-Yan Chang, Yau-Tsz Lai, Tianfan Cheng, Haibo Wang, Ya Yang and Hongzhe Sun[*]

Department of Chemistry, The University of Hong Kong, Pokfulam Road, Hong Kong, P. R. China.

*Corresponding author: Fax: (+852) 2857 1586; Tel: (+852) 2859 8974; E-mail: hsun@hku.hk

Abstract: Hpn-like (Hpnl) is a unique histidine- and glutamine-rich protein found only in *Helicobacter pylori* and plays a role on nickel homeostasis. We constructed the fluorescent sensor proteins *CY*Hpnl and *CY*Hpnl_1-48 (C-terminal glutamine-rich region truncated) using enhanced cyan and yellow fluorescent proteins (eCFP and eYFP) as the donor-acceptor pair to monitor the interactions of Hpnl with metal ions and to elucidate the role of conserved Glu-rich sequence in Hpnl by fluorescence resonance energy transfer (FRET). *CY*Hpnl and *CY*Hpnl_1-48 exhibited largest responses towards Ni(II) and Zn(II) over other metals studied and the binding of Bi(III) to *CY*Hpnl was observed in the presence of excess amount of Bi(III) ions (K_d= 115 ± 4.8 μM). Moreover, both *CY*Hpnl and *CY*Hpnl_1-48 showed positive FRET responses towards the binding to Ni(II) and Zn(II) in *E. coli* cells overexpressing *CY*Hpnl and *CY*Hpnl_1-48, whereas a decrease in FRET upon Bi(III)-binding in *E. coli* cells overexpressing the latter. Our study provides clear evidence on Hpnl binding to nickel in cells, and intracellular interaction of Hpnl with Bi(III) could disrupt the protein function, thus probably contributing to the efficacy of Bi(III) drugs against *H. pylori*.

1. Introduction

Helicobacter pylori resides in acidic gastric environment and infects more than 50% of the world population, leading to peptic ulcer and even gastric cancer [1,2]. Two nickel-containing metalloenzymes, [NiFe] hydrogenase [3,4] and urease [5-7], are essential for the survival and colonization of *H. pylori* under extremely low pH condition [8]. Intracellular level of nickel is thus tightly regulated in uptake, trafficking, storage and release, accounting to its necessity and toxicity [7,9,10]. Histidine-rich Hpn and histidine- and glutamine-rich Hpn-like (Hpnl) proteins have been found to serve as nickel reservoirs in *H. pylori*, which supply the metal for the maturation of hydrogenase and urease (Table S4-S5) [6,11-14]. In scarce nickel condition, wild-type *H. pylori* colonizes more efficiently in mice than both *hpn* and *hpnl* gene deleted *H pylori*, pinpointing the

importance of Hpn and Hpnl in *H. pylori* colonization under its physiological condition [15]. Although the role of Hpnl has been proposed, its interaction with metal ions in actual cellular environment has not been clearly demonstrated.

Bismuth-based medications, such as colloidal bismuth subcitrate (DeNol®, Lizhudele®), bismuth subsalicylate (Pepto-Bismol®) and ranitidine bismuth citrate (Pylorid®), have been used for the treatment of microbe-causing gastrointestinal infections for decades, in particular to eradicate *H. pylori* infection when combined with antibiotics [16-20]. Proteins, especially enzymes, are believed to be the therapeutic targets although the molecular mechanism of bismuth drugs is not fully understood and the intracellular monitoring of drug actions is still lacking [5,15,17].

Fluorescence resonance energy transfer (FRET) has been widely used to examine the reaction kinetics through monitoring the conformational changes of biomolecules upon their interactions with corresponding substrates [21-23]. Fluorescent proteins frequently serve as FRET donor-acceptor pairs given that they can be genetically-encoded to the proteins of interest, and the fusion proteins are expressed for fluorescence studies inside cells [24,25]. Moreover, genetically-encoded FRET sensors can also be used to elucidate the concentration of metal ions in cells, owing to their abilities of accurately targeting various subcellular organelles [24,26,27].

In this work, we engineered a fluorescent sensor protein *CY*Hpnl to examine the interaction of Hpnl towards various metal ions by FRET, utilizing eCFP and eYFP as the FRET donor-acceptor pair. To investigate the role of highly conserved C-terminal glutamine-rich sequence, a mutant of *CY*Hpnl (*CY*Hpnl_1-48) was constructed and similar study was carried out. We further explored the metal-binding properties of Hpnl by overexpressing *CY*Hpnl or *CY*Hpnl_1-48 in bacterial cells. The metal selectivity of Hpnl *in vitro* and in cells is compared and the effect of bismuth drug is discussed.

2. Experimental

2.1 Materials

Primers were synthesized by Life Technologies. All chemicals were purchased from Sigma-Aldrich or USB, and were used without further purification.

2.2 Construction of pET32a-eCFP-Hpnl-eYFP and C-terminal glutamine-deleted mutant pET32a-eCFP-Hpnl_NoCterQ-eYFP expression vectors

The full-length *ecfp* and *eyfp* genes were PCR-amplified from plasmids pECFP-Nuc and pEYFP-C1 (Clontech Laboratories) by primer pairs (CFP-For/CFP-Rev and YFP-For/YFP-Rev). The *hpnl* gene was amplified from *H. pylori* 11637 genomic DNA using primer Hpnl-For/Hpnl-Rev (Table S1). After digestion by corresponding restriction endonucleases (New England Biolabs), the PCR products *ecfp* and *eyfp* were successively inserted into pET32a vector to obtain the plasmid pET32a-eCFP-eYFP and hpnl gene was inserted between *ecfp* and *eyfp* genes to obtain the plasmid pET-eCFP-Hpnl-eYFP (named pET-*CY*Hpnl hereafter). Linkers with a sequence of Gly-Ser-Gly-Ser were inserted among the genes of *ecfp*, *hpnl* and *eyfp* to enhance the flexibility and solubility of

the sensors.

For the C-terminal glutamine-deleted mutant pET32a-eCFP-Hpnl_1-48-eYFP (named pET-*CY*Hpnl_1-48 hereafter), *hpnl* gene was amplified with primer pair (Hpnl-For/Hpnl-NoCQ-Rev) and the mutant *hpnl* gene was inserted into pET32a-eCFP-eYFP plasmid. Plasmid pET28a-eCFP-eYFP (named pET-*CY*FP hereafter) was also constructed to produce a fluorescent sensor protein consisting of only the flexible linker (Gly-Ser-Gly-Ser) between the genes of eCFP-eYFP FRET donor-acceptor pair for control experiments.

2.3 *Expression and purification of CYHpnl and CYHpnl_1-48*

Plasmids pET-*CY*Hpnl and pET-*CY*Hpnl_1-48 were transformed into *Escherichia coli* BL21(DE3). The overnight culture was subcultured into fresh Luria-Bertani (LB) medium with 1:100 dilution supplemented with 100 μg/ml ampicillin and was grown at 37 °C until OD_{600} reached 0.6. Protein expression was induced overnight at 25 °C in the presence of 0.2 mM isopropyl β-D-1-thiogalactopyranoside (IPTG). Bacterial pellets were harvested by centrifugation and resuspended in buffer A (20 mM Tris-HCl, pH 7.6, 500 mM NaCl, and 1 mM tris(2-carboxyethyl)phosphine hydrochloride (TCEP)) supplemented with 1 mM phenylmethylsulfonyl fluoride (PMSF).

Cells were lysed by sonication, then the lysates was centrifuged at 10,000 *g* at 4 °C for 30 minutes and the supernatant was applied to HisTrap HP column (GE Healthcare). The column was washed with buffer A in the presence of increasing amount of imidazole (from 20 to 150 mM) and the protein was eluted with buffer A containing 200 mM imidazole. Fractions were collected and were analysed by 12% sodium dodecyl sulphate-polyacrylamide gel electrophoresis (SDS-PAGE) (Fig. S1). The peak fraction was further purified by Resource Q column (GE Healthcare) with a linear gradient of NaCl from 0 to 500 mM and the peak fractions were pooled and dialyzed against Buffer B (10 mM 2-(*N*-morpholino)ethanesulfonic acid (MES), pH 6.8, 150 mM $(NH_4)_2SO_4$) three times at 4 °C for six hours for subsequent use. Protein concentration was determined by BCA Protein Assay Kit (Novagen). ICP-MS analysis (Agilent 7500a spectrometer) was performed to ensure the protein remained as an apo-form prior to fluorescence analysis.

2.4 *In vitro FRET analysis*

Full fluorescence emission spectra were obtained on a Hitachi F7000 Fluorescence Spectrophotometer using 1 cm x 1 cm quartz cuvette. *CY*Hpnl (250 nM in Buffer B) was excited at 433 nm with 1000 W xenon lamp source at the excitation and emission slit width of 5 nm. The photomultiplier voltage was set to be 650 V and emission spectra were scanned from 450 to 650 nm at a speed of 40 nm per second.

Fluorescence experiments were carried out on a Beckman Coulter DTX880 Multimode Detector, using the excitation filter 405/30 nm and emission filter 465/30 nm and 535/30 nm. Intensity ratio of the two emission signals (emission ratio= 535/30: 465/30) was used to quantify the FRET changes. Metal stock solutions were prepared from $NiSO_4$, $ZnSO_4$, $CoSO_4$, $MnSO_4$, $MgSO_4$, $CuSO_4$ and $Bi(NO_3)_3$ (in glycerol). Molar equivalents of various metal ions were added to

400 nM of *CY*Hpnl or *CY*Hpnl_1-48 or *CY*FP (as a control) in Buffer B. The changes in FRET emission ratio (emission at filters 535/30:465/30) were calculated by averaging the results of at least three replicates.

2.5 Metal-binding capacities of CYHpnl

The dissociation constants (K_d) for Ni(II)- and Zn(II)-*CY*Hpnl were determined by equilibrium dialysis. Apo-*CY*Hpnl (20 μM) solution was filled into home-made dialysis tubes (3 kDa cutoff) and was dialyzed against Buffer B supplemented with a series of concentrations of Ni(II) and Zn(II) ions overnight at 4°C. ICP-MS was employed to determine the metal concentrations in and outside the dialysis tubes while nonlinear fitting with Hill equation in GraphPad Prism 5 ($Y = B_{max}*X\wedge h / (K_d\wedge h + X\wedge h)$, where B_{max} is the maximum specific binding, h is the Hill coefficient and K_d is the dissociation constant) was used to calculate the dissociation constant (K_d) for Ni(II)- and Zn(II)-binding to *CY*Hpnl after normalization with protein concentration.

To determine the K_d of Bi(III) to *CY*Hpnl, nonlinear fitting with Hill equation in GraphPad Prism 5 ($Y = B_{max}*X\wedge h / (K_d\wedge h + X\wedge h)$)) was employed to analyze the FRET results with titration of Bi to *CY*Hpnl. To determine the stoichiometries of metal binding to *CY*Hpnl, *CY*Hpnl (20 μM) was incubated with six molar equivalents of Ni(II), Co(II), Cu(II) Zn(II) and Bi(III) and excess metal ions were removed by buffer exchange prior to ICP-MS analysis.

2.6 FRET analysis in E. coli cells

Plasmid pET-*CY*Hpnl or pET-*CY*Hpnl_1-48 was transformed into BL21(DE3) *E. coli* cells. An overnight culture was inoculated into fresh LB medium in the presence of 100 μg/ml ampicillin. Cells were harvested by centrifugation at 4,000 rpm when OD_{600} reached 0.6 and were subsequently washed three times with freshly prepared MOPS minimal medium [28] containing 100 μg/ml ampicillin. Cells were then grown at 37 °C in MOPS minimal medium for 30 minutes after washing for recovery. Protein expression was induced at 25 °C for at least 16 hours with the use of 0.2 mM IPTG. The OD_{600} of bacterial culture was measured and subsequently diluted to the OD_{600} of 0.4. Various concentrations of Ni(II), Zn(II) and Bi(III) ions (as colloidal bismuth subcitrate), ranged from 0 to 200 μM, were then added to the bacterial cell culture medium for four-hour incubation at 25 °C prior to fluorescence measurement. Samples were subjected to Beckman Coulter DTX880 Multimode Detector for fluorescence measurement with the same setting as in *in vitro* FRET experiments. *CY*FP-overexpressed *E. coli* cells were also subjected to FRET analysis after four-hour incubation with Ni(II), Zn(II), Mg(II) and Bi(III) (0 - 200 μM) as a control.

3. Results

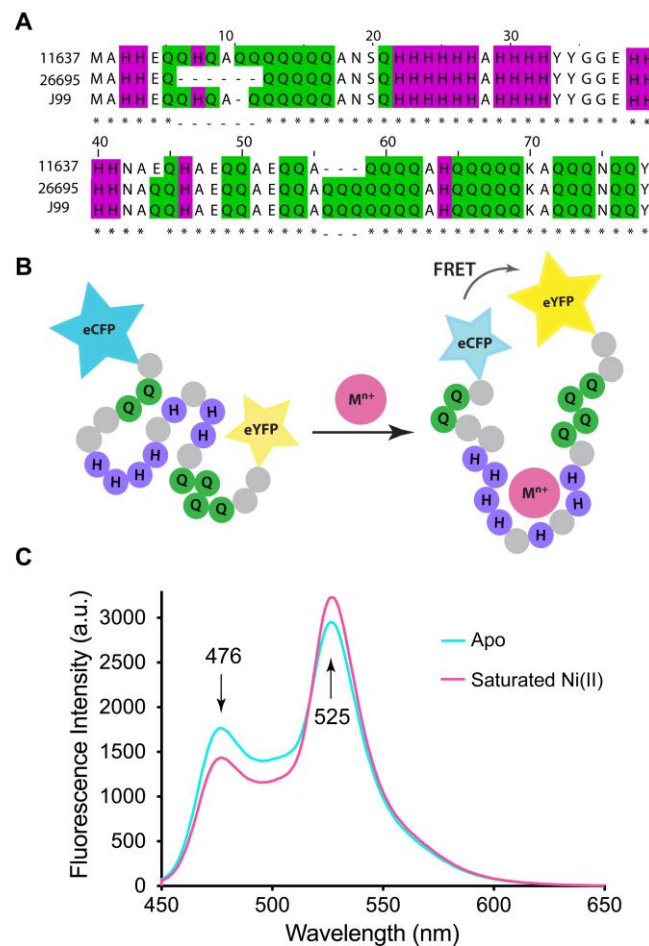## 3.1 Detection of metal binding by FRET and in vitro metal selectivity and affinity of CYHpnl

Fig. 1 (A) Sequence alignment of three strains of *H. pylori* by MUSCLE (Jalview) [29], showing the highly-conserved histidine- (*purple*) and glutamine (*green*) residues in Hpnl. (B) Both full length and C-terminal-truncated Hpnl sequence were inserted between the FRET partners, eCFP and eYFP. Conformational changes were induced upon the interaction with metal ions. (C) Fluorescence spectra of *CY*Hpnl in the absence and presence of Ni(II) ions (λ_{ex} = 433 nm).

The strategy for the design and fabrication of the fluorescent sensor proteins are illustrated in Fig. 1B. We first investigated the occurrence of FRET between eCFP and eYFP due to the conformational change in the target Hpnl protein by fluorescence spectroscopy using purified *CY*Hpnl. Addition of Ni(II) ions to *CY*Hpnl led to a decrease in the eCFP fluorescence at 476 nm and an increase in the eYFP fluorescence (525 nm), with gradual changes in the eCFP and eYFP fluorescence emission upon the titration of increasing amount of Ni(II) ions, demonstrating the metal concentration-dependent change in FRET signals (Fig. 1C and Fig. S3). This is due to the conformational change of the Hpnl protein induced by Ni(II), resulting in a reduction in the distance between eCFP-eYFP FRET donor-acceptor pair. The quenching of eCFP fluorescence was

accomplished by the transfer of energy to the proximate eYFP molecule, leading to the decline in eCFP fluorescence and an upsurge of eYFP fluorescence in comparison with the apo-form of *CY*Hpnl. Consequently, FRET efficiency can be quantified by the change in the FRET emission ratio (I_{525}/I_{476}). Metal binding to the target *CY*Hpnl and *CY*Hpnl_1-48 proteins can be detected by FRET, more specifically by the change in FRET ratio.

Previously, it has been demonstrated that Hpnl binds to Ni(II), Cu(II), Co(II) and Zn(II) with micromolar affinity (Table S5) [12]. To investigate the metal selectivity of the protein, *CY*Hpnl (400 nM) was incubated with various metal ions (up to 2.4 µM), including Cu(II), Ni(II), Zn(II), Co(II), Mn(II), Mg(II) and Bi(III), and was subjected to fluorescence analysis as described in experimental section. Apparent increase in the FRET ratios were observed for Ni(II) and Zn(II) and the increase in the amount of these metals led to further enhancement of FRET ratio (Fig. 2). Maximum changes of approximately 35% and 20% in the FRET ratio were observed for Ni(II) and Zn(II) respectively. In contrast, less than 5% changes in the FRET ratio of *CY*Hpnl were recorded for Cu(II), Co(II), Mn(II) and Bi(III) ions, which were similar to that of the control metal ions (i.e. Mg(II)). FRET analysis with the control *CY*FP showed little changes in FRET, indicating that the metal-induced FRET in *CY*Hpnl was due to the interaction between metal and protein of interest Hpnl (Fig. S4). Circular dichroism (CD) was performed to investigate the changes in secondary structure of *CY*Hpnl upon metal titration (Supporting information). It was found that apparent changes in secondary structure were induced upon interaction with Ni(II), followed by Zn(II), possibly elaborating the greatest change in FRET responses upon Ni(II) and Zn(II) titration (Fig. S5). Based on the FRET results, we concluded that Ni(II)- and Zn(II)-binding to *CY*Hpnl can be selectively monitored by FRET but not other metal ions studied.
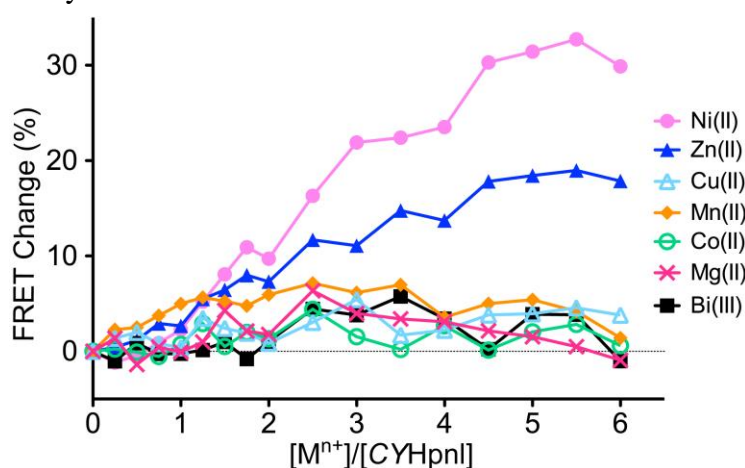

Fig. 2 Changes (%) in FRET ratio of *CY*Hpnl (400 nM) upon the addition of different molar equivalents of metal ions.
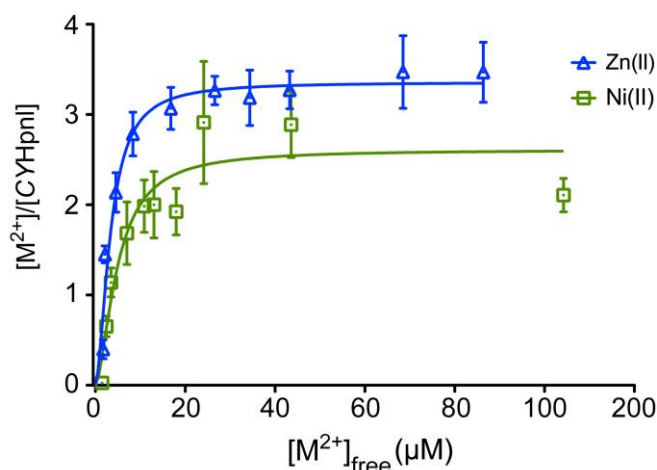
Fig. 3 Binding of *CY*Hpnl to Ni(II) and Zn(II) by equilibrium dialysis. The data were fitted with Hill equation.

To quantify the binding affinities of *CY*Hpnl to Ni(II) and Zn(II), equilibrium dialysis was applied by supplementing Ni(II) and Zn(II) to the apo-protein and the results were analysed by non-linear fitting with Hill equation (Fig. 3). *CY*Hpnl was found to bind 2.5 ± 0.1 Ni(II) with the dissociation constants (K_d) of 4.6 ± 0.7 μM with cooperativity (h = 1.77 ± 0.37). *CY*Hpnl bound 3.3 ± 0.1 Zn(II) and the dissociation constants (K_d) was estimated to be 3.4 ± 0.4 μM with cooperativity (h = 1.75 ± 0.36) (Fig. 3). The cooperativity (where h~ 2) detected might confirm that approximately two binding sites with certain extent of cooperativity are involved in Ni- and Zn-binding to *CY*Hpnl [30]. It was revealed that *CY*Hpnl possesses similar binding affinities towards Ni(II) and Zn(II), comparable to those of native Hpnl [12]. Further analysis by ICP-MS confirmed that *CY*Hpnl binds 2.2 ± 0.1 Ni(II) and 2.1 ± 0.2 Zn(II) (Table S2), almost identical to those of native Hpnl. It was, however, noted a discrepancy between the results in equilibrium dialysis and ICP-MS analysis in Zn-binding to *CY*Hpnl. As it has been previously validated that Hpnl can only bind two Zn(II) [12], the extra Zn(II) ions associated with *CY*Hpnl could thus be postulated to be possible weak non-specific interaction of Zn(II) with the fluorescent proteins. Nevertheless, the incorporation of eCFP and eYFP appeared to have little effect on the metal binding affinities of Hpnl to Ni(II) and Zn(II).

3.2 Interaction between CYHpnl and Bi(III)

The N-terminus of Hpnl shares more than 50% sequence identity with that of Hpn in *H. pylori* (Fig. S9), which has been demonstrated to contribute to the Bi(III) tolerance by sequestering therapeutic Bi(III) drugs [14,31]. A previous FRET study demonstrated that the presence of bismuth in great surplus relative to the protein (at least an excess of 200-fold) was required to induce FRET responses in Bi(III)-binding Hpn *in vitro* [21]. To further examine whether *CY*Hpnl binds Bi(III) ions, increasing amount of Bi(III) ions (as Bi(NO$_3$)$_3$ for up to 320 μM) was titrated into the purified *CY*Hpnl (400 nM) and the changes in FRET signals were recorded.
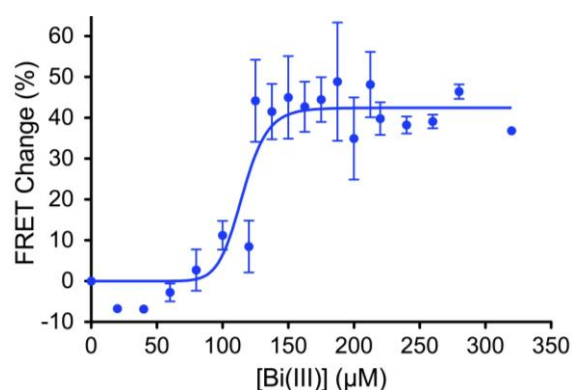
7

Fig 4. Binding of Bi(III) to *CY*Hpnl. An increase in FRET signal was not observed until the addition of 80 μM of Bi(III) ions to *CY*Hpnl (400 nM). The data were fitted by the Hill equation.

No FRET signals were detected when low concentrations of Bi(III) ions were added to *CY*Hpnl (400 nM). However, to our surprise, addition of 80 μM of Bi(III) led to observable FRET signals, which further increased by about 40% and reached a plateau at Bi(III) concentration of 120 μM (Maximum FRET change, B_{max} = 42.5 ± 2.2%). The binding curve was fitted by Hill equation to give rise to a dissociation constant (K_d) of 115.3 ± 4.8 μM with cooperativity (h = 12.2 ± 5.0), indicative of a very weak binding, much weaker than Hpn (Fig. 4) [21]. It has been pinpointed that the Hill coefficient could only reflect the minimal ligand binding sites in ligand-receptor interaction [30]. From the hill coefficient obtained from the fitting with Hill equation, approximately twelve binding sites with certain cooperativity were involved in Bi-binding to *CY*Hpnl. To further monitor Bi(III)-binding to *CY*Hpnl, column-based gel electrophoresis coupled with ICP-MS (GE-ICP-MS) was used according to our previous report (Supporting information) [32]. Upon incubation of 120 μM of Bi(III) (as $Bi(NO_3)_3$) for an overnight, *CY*Hpnl was loaded onto column-based gel electrophoresis for the measurement of the [209]Bi profile by ICP-MS whereas the molecular weight of the corresponding protein was calibrated by iodinated protein markers simultaneously. The evident bismuth signal observed at ~ 75 kDa confirming that *CY*Hpnl binds Bi(III) at high Bi(III) concentration (Fig. S7D), indicative of the potentially specific binding of Bi(III) to Hpnl.

3.3 Effect of glutamine residues on metal-CYHpnl interactions

Analysis on the sequences of three strains of *H. pylori* showed that the consecutive glutamine residues in Hpnl are highly conserved (Fig. 1A). The glutamine residues have been demonstrated to be able to stabilize metal ions in the binding site due to hydrogen bonding [33,34]. To understand the effect of the glutamine-rich sequence located at the C-terminus of Hpnl on its metal-binding properties, a mutant with the C-terminal glutamine-rich region truncated *CY*Hpnl, i.e. *CY*Hpnl_1-48, was constructed and similar experiments were performed with the purified protein.

Similar to *CY*Hpnl, incubation of increasing amount of Ni(II) and Zn(II) (up to 6 molar equivalents) with *CY*Hpnl_1-48 resulted in maximum changes of about 30% and 20% in the FRET ratio, respectively (Fig. 5). Addition of different molar equivalents of Cu(II) produced a slight decrease in FRET ratio of about 10%, which might also suggest a possible interaction between *CY*Hpnl_1-48 and Cu(II). Less than 5% changes in the FRET ratio were observed for Co(II), Mg(II), Mn(II) and Bi(III). Ni(II) and Zn(II) again induced the largest FRET responses (20% and 30% respectively) in *CY*Hpnl_1-48, indicating that the glutamine-rich C-terminus of Hpnl plays a little role in terms of metal-binding *in vitro*.
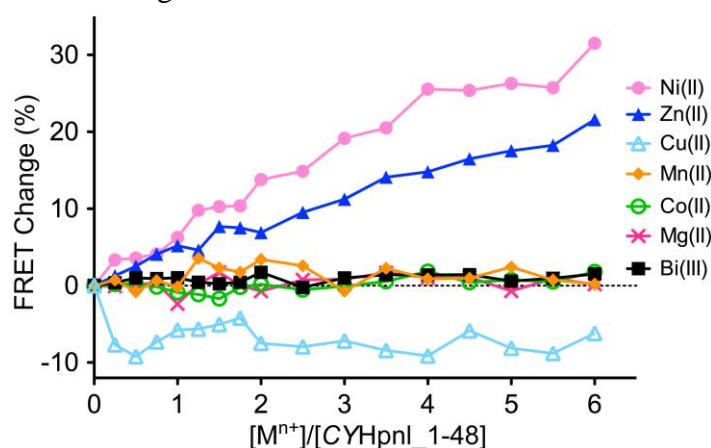

Fig 5. Changes (%) in FRET ratio upon the addition of different molar equivalents of metal ions to purified *CY*Hpnl_1-48 (400 nM). Note the evident changes of FRET induced by Ni(II) and Zn(II).

3.4 Metal selectivity of CYHpnl and CYHpnl_1-48 in cells

To examine the metal selectivity of *CY*Hpnl in cells, we performed similar experiments in live *E. coli* cells. *CY*Hpnl-overexpressing cells were cultured in minimal medium supplemented with the target metal ions. No toxicity was observed within the working concentration of all added metal ions as reflected from the optical density at 600 nm. Upon incubation with Ni(II), Zn(II) and Bi(III) ions (as colloidal bismuth subcitrate) for four hours, FRET changes were detected from 50 µM of Ni(II), Zn(II) and Bi(III) in *CY*Hpnl-overexpressed *E. coli* and were saturated at about 100 µM of all metal ions. Significant changes in FRET ratio were observed for Ni(II) and Zn(II) ions with around 20% increase in FRET ratio for both metal ions ($P < 0.05$, analyzed by unpaired *t*-test; two-tailed) (Fig. 6A). Approximately 10% change in FRET ratio was observed for Bi(III). Similar to *in vitro* studies, *CY*Hpnl exhibited a higher selectivity towards Ni(II) and Zn(II) intracellularly. Analysis of FRET in *CY*FP-overexpressed cells showed that there was no evident FRET signals (about 5%), indicating that the FRET responses were resulted from the metal binding to Hpnl, but not due to non-specific interaction with the sensor protein itself (Fig. S8).
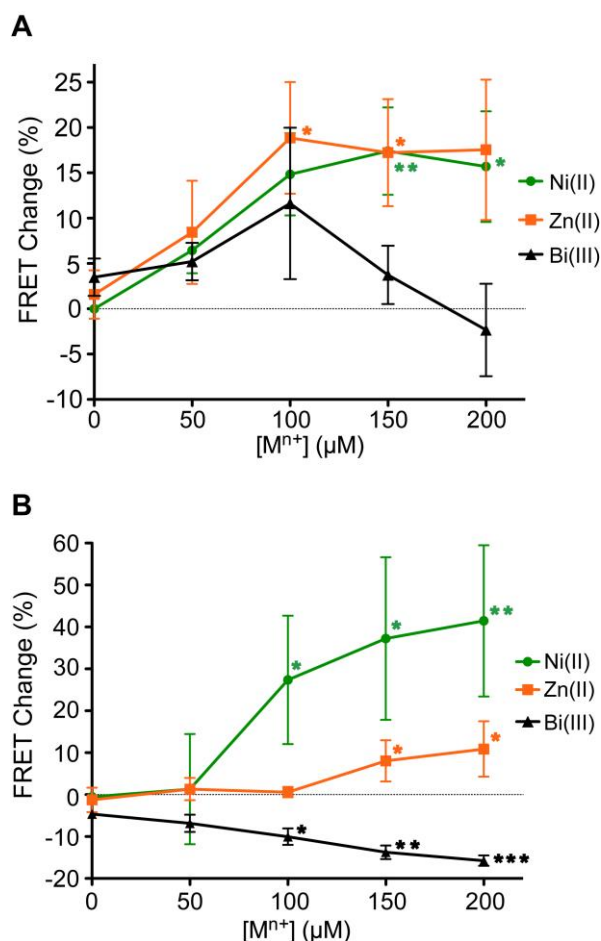
Fig. 6 Changes (%) in FRET ratio after the incubation with different metal ions in (A) *CY*Hpnl and (B) *CY*Hpnl_1-48 overexpressed *E. coli*. Data were analyzed by unpaired *t*-test; two-tailed with $P < 0.05$ as indicated by the asterisks on the figure.

We showed that the deletion of C-terminal glutamine-rich sequence did not alter the metal-binding properties of *CY*Hpnl significantly (Fig. 5). We evaluated the metal selectivity of *CY*Hpnl_1-48 in *E. coli* cells under identical conditions (Fig. 6B). Similar to *CY*Hpnl protein, the largest increase in FRET ratio was observed upon the addition of Ni(II) to the cell culture medium (about 40%), indicating that the deletion of C-terminal glutamine-rich residues does not alter Ni(II) coordination to Hpnl protein. Intriguingly, addition of Zn(II) or Bi(III) ions resulted in decline in the FRET ratio, in particular about 20% negative FRET change for Bi(III), in contrast to the results obtained for the *CY*Hpnl, suggesting that the C-terminal glutamine residues may play a role in metal binding inside cells.

To confirm that the FRET responses observed *in vivo* were due to the coordination of metal ions to *CY*Hpnl (and *CY*Hpnl_1-48), but not resulted from the disturbance of cellular metal homeostasis, the culture medium after protein overexpression was treated with EDTA (Supporting information). It has been reported previously that metal chelators like EDTA may increase the outer membrane permeability of gram-negative bacteria, facilitating some impermeable molecules to

cross the cell membrane [35]. Metal homeostasis would then be disturbed by EDTA treatment, after which its effects on FRET could be revealed. Less that 5% changes in FRET ratio were noticed after EDTA treatment (Fig. S6), demonstrating the negligible effect on FRET by the trace metal ions in culture medium.

To further validate the coordination of Bi(III) to *CY*Hpnl_1-48 in cells, GE-ICP-MS was employed similarly [32] (Supporting information). To eliminate the background of Bi(III)-binding proteins in cells, *E. coli* cells with *CY*FP-overexpression was constructed and incubated with Bi(III) similarly prior to analysis of metals in cell lysates by GE-ICP-MS as a control. Two major ^{209}Bi peaks were observed in the GE-ICP-MS profile of *CY*FP-overexpressed *E. coli* with molecular weights of about 29 and 50 kDa (Fig. S7A), indicative of potential Bi(III)-binding proteins in *E. coli* cells. However, there was no ^{209}Bi peaks at molecular weight ~ 75 kDa. In contrast, a distinct peak at about 75 kDa was observed in GE-ICP-MS profile of cell lysate of *CY*Hpnl_1-48-overexpressed cells in addition to two ^{209}Bi peaks corresponding to molecular weights of about 29 and 50 kDa (Fig. S7B).

4. Discussion

Many lower organisms including *H. pylori* require Ni(II) for specific functions. However, excessive Ni(II) ions are toxic to organisms. Given that *H. pylori* colonizes stomach where it is highly acidic, the proper functions of two Ni(II)-containing enzymes, urease and [Ni,Fe] hydrogenase, are crucial for the survival and colonization of the bacterium. The bacterium synthesizes two small and unique proteins, histidine-rich Hpn and histidine- and glutamine-rich Hpnl, for nickel storage and detoxification, similar to the functions of other histidine-rich proteins [11,13,15]. Histidine-rich proteins or histidine-rich motifs have also been shown to play a key role in metal homeostasis in a broad spectrum of bacterial species in a habitat-related manner [36]. Previous *in vitro* experiments have demonstrated that both Hpn and Hpnl bind to Ni(II) strongly and reversibly [11,13]. In addition, Hpn was shown to bind Bi(III) both *in vitro* and *in vivo* and might serve as one of the Bi(III) drug targets [14,21,31].

In the present study, we constructed FRET sensors, *CY*Hpnl and *CY*Hpnl_1-48, based on a previous report [21]. Gradual changes in FRET were shown upon the addition of increasing amount of metal ions in *in vitro* and in intracellular studies, providing a solid elaboration of the FRET analyses. We found that protein *CY*Hpnl binds two Ni(II) and two Zn(II) ions *in vitro* by ICP-MS (Table S2) with the dissociation constants at micromolar level as determined by equilibrium dialysis, despite the presence of weak non-specific interaction between Zn(II) and fluorescent proteins revealed in equilibrium dialysis (Fig. 3). The binding affinities of Ni(II) and Zn(II) to *CY*Hpnl were similar to those of the native Hpnl protein (Table S5) [12]. No oligomeric state of *CY*Hpnl and *CY*Hpnl_1-48 was observed upon incubation with Ni(II), Zn(II) and Bi(III), confirming that the FRET changes were merely owing to the conformational changes of the proteins (Fig. S2). Importantly, evident changes of fluorescence (FRET ratio) in *E. coli* cells

11

overexpressing *CY*Hpnl and *CY*Hpnl_1-48 were observed in the presence of Ni(II) and Zn(II). In contrast, trivial changes for Co(II), Cu(II) and Mn(II) were observed (data not shown), indicative of intracellular binding of *CY*Hpnl to Ni(II) and Zn(II). These results are in agreement with the proposed functions of Hpnl in *H. pylori* [11,12,15]. It has also been shown that Ni(II) induced the largest change in secondary structure in native Hpnl protein [12], which is also demonstrated in the CD spectra of *CY*Hpnl (Fig. S5), i.e., the greatest conformational changes of *CY*Hpnl were induced by Ni(II). The higher selectivity of *CY*Hpnl towards Ni(II) ions observed in this FRET study may be related to the conformation of the intrinsic metal-binding sites of Hpnl that are structurally favourable towards specific metal ions.

Different from Hpn, Hpnl has unique glutamine-rich motifs, whose role remains unclear (Fig. S9). We, therefore, engineered a C-terminal glutamine truncated mutant (*CY*Hpnl_1-48) to investigate the role of these highly conserved glutamine residues in Hpnl. Deletion of the C-terminal glutamine residues did not lead to significant differences in FRET signals for all the metal ions studied *in vitro*, indicating that these glutamine residues might not be involved in direct binding to metal ions. Surprisingly, the changes of FRET ratio *in vivo* for *CY*Hpnl_1-48 upon incubation with Ni(II) were doubled comparing with that of *CY*Hpnl under similar conditions. Moreover, the interaction of *CY*Hpnl_1-48 and Bi(III) ions in cells was disclosed with the FRET signals being significantly different from those without any added metal ions (Fig. 6). Glutamine-rich motifs in proteins have been found to be involved in the reversible interaction between proteins, and their roles in facilitating protein oligomerization have also been suggested [34,37-39]. The glutamine-rich sequences in Hpnl might indirectly enhance the protein folding, introducing certain degree of rigidity in the structure of native Hpnl. Larger change in conformation might therefore be observed in the glutamine-rich sequence truncated mutant *CY*Hpnl_1-48. Further biological investigation on the role of the glutamine-rich sequences of Hpnl would therefore appear to be warranted.

Although Hpn was shown to bind Bi(III) both *in vitro* and *in vivo*, there appears no reports on whether Hpnl interacts with Bi(III). We showed here that similar to the FRET-based study on Hpn [21], titration of up to six molar equivalents of Bi(III) to *CY*Hpnl did not show significant FRET signals until high Bi(III) concentration, indicative of a weaker binding of Hpnl towards Bi(III) than Hpn as reflected from their binding affinities. This may be attributed to the fact that Hpnl protein lacks cysteine pairs which are usually favoured by the metal [40]. Unexpectedly, negative changes in FRET were detected when increasing amount of Bi(III) ions were incubated with the *CY*Hpnl_1-48-overexpressed cells. Similar negative changes in FRET have been reported previously [25,41,42], attributing to an increase in the distance between eCFP-eYFP FRET donor-acceptor pair upon protein-substrate interaction. The negative FRET signals observed in *CY*Hpnl_1-48-overexpressed cells may imply the interaction of *CY*Hpnl_1-48 with Bi(III) ions. As confirmed by a home-made GE-ICP-MS, the distinct Bi(III) peak at approximately 75 kDa observed exclusively in [209]Bi profile of cell lysate of *CY*Hpnl_1-48-overexpressed cells (as well as *CY*Hpnl-overexpressed cells, Fig. S7B-C) whereas was absence in *CY*FP-overexpressed *E. coli* cells (i.e. without

*CY*Hpnl_1-48 and *CY*Hpnl overexpression) under identical conditions, validating the intracellular binding of Bi(III) to both *CY*Hpnl_1-48 and *CY*Hpnl (Fig. S7A-C). Discrepancy in FRET responses between Bi(III) and other metal ions in *in vivo* suggested different conformational changes (or existence of distinctive binding sites) upon Bi(III) binding to *CY*Hpnl. However, caution shall be taken that metal homeostasis in *H. pylori* may be different from that of the model bacterium *E. coli*. Nevertheless, FRET analyses on metal interaction with Hpnl in native organism *H. pylori* may be beneficial for future investigation.

This study provides comprehensive investigation of metal-binding properties of Hpnl *in vitro* and in cells although the FRET results might not represent all metal-*CY*Hpnl interaction. Neither Co(II) nor Cu(II) binding to *CY*Hpnl nor intracellular Bi(III)-binding to *CY*Hpnl produced noticeable FRET signals (Table S2, Fig. S7A and S7C), which might be attributed to the limited conformational changes of the protein induced by the metals as shown in CD spectra (Fig. S5). Besides, the difference in oligomeric state between native Hpnl (as a 22-mer as reported in [11]) and *CY*Hpnl (as a monomer as shown in Fig. S2 in this report) might lead to deviation in metal-binding properties between native Hpnl and the fluorescent sensor protein *CY*Hpnl. Examinations by other techniques, such as GE-ICP-MS, were thus used to compare with FRET results. Nevertheless, FRET analyses signify an indirect method to scrutinize protein-substrate interactions, confining to the conformational changes induced during interaction.

5. Conclusion

*CY*Hpnl and *CY*Hpnl_1-48 were constructed to investigate the interaction of Hpnl and Hpnl_1-48 with metal ions. Binding to Ni(II) and Zn(II) resulted in the largest changes in FRET ratio and the dissociation constants were determined to be 4.6 and 3.4 μM respectively. Ni(II) and Zn(II) also interact with *CY*Hpnl and *CY*Hpnl_1-48 in overexpressed bacterial cells. Our comparative FRET study for both *CY*Hpnl and *CY*Hpnl_1-48 indicated that the glutamine-rich C-terminus did not participate in direct coordination with metal ions although it might affect the metal-binding properties of Hpnl. The selectivity of *CY*Hpnl towards Ni(II) both *in vitro* and *in vivo* elucidated the important role of Hpnl for sequestering nickel in *H. pylori*. Very weak but specific interaction of *CY*Hpnl with Bi(III) was found. Negative FRET changes were observed after incubation with Bi(III) in cellular condition and binding of Bi(III) to *CY*Hpnl in cells was confirmed by GE-ICP-MS, indicative of different binding mode of Bi(III) compared with other metal ions. Finally, the FRET approach enables metal-protein interactions to be monitored directly in cells, offering a useful method for metalloproteomics [16,43].

Abbreviations

FRET	Fluorescence Resonance Energy Transfer
Hpnl	Hpn-like
CFP/YFP	Cyan fluorescent protein / Yellow fluorescent protein
*CY*Hpnl	Sensor protein with full-length *hpnl* gene inserted between *ecfp* and *eyfp* gene

*CY*Hpnl_1-48	Sensor protein with C-terminal glutamine-rich region truncated *hpnl* gene inserted between *ecfp* and *eyfp* gene
*CY*FP	Sensor protein with only eCFP and eYFP FRET donor-acceptor pair
IPTG	β-D-1-isopropyl thiogalactopyranoside
TCEP	Tris(2-carboxyethyl)phosphine hydrochloride
PMSF	Phenylmethylsulfonyl fluoride
MES	2-(*N*-morpholino)ethanesulfonic acid
GE-ICP-MS	Column-type gel electrophoresis coupled with inductively coupled plasma mass spectrometry

Appendix A. Supplementary data

Supplementary data to this article can be found online (XXXXX)

References

[1] A. Covacci, J.L. Telford, G.D. Giudice, J. Parsonnet, R. Rappuoli, Science 284 (1999) 1328-1333.

[2] J.G. Kusters, A.H. van Vliet, E.J. Kuipers, Clin. Microbiol. Rev. 19 (2006) 449-490.

[3] J.W. Olson, R.J. Maier, Science 298 (2002) 1788-1790.

[4] R.J. Maier, C. Fu, J. Gilbert, F. Moshiri, J. Olson, A.G. Plaut, FEMS Microbiol. Lett. 141 (1996) 71-76.

[5] R.J. Maier, S.L. Benoit, S. Seshadri, Biometals 20 (2007) 655-664.

[6] S. Seshadri, S.L. Benoit, R.J. Maier, J. Bacteriol. 189 (2007) 4120-4126.

[7] Y. Li, D.B. Zamble, Chem. Rev. 109 (2009) 4617-4643.

[8] K.A. Higgins, C.E. Carr, M.J. Maroney, Biochemistry 51 (2012) 7816-7832.

[9] H. de Reuse, D. Vinella, C. Cavazza, Frontiers in cellular and infection microbiology 3 (2013) 94, doi: 10.3389/fcimb.2013.00094.

[10] A.M. Sydor, D.B. Zamble, Metal Ions Life Sci. 12 (2013) 375-416.

[11] Y. Zeng, D. Zhang, H. Li, H. Sun, J. Biol. Inorg. Chem. 13 (2008) 1121-1131.

[12] Y. Zeng, N. Yang, H. Sun, Chem. Eur. J. 17 (2011) 5852-5860.

[13] R. Ge, R.M. Watt, X. Sun, J.A. Tanner, Q. He, J. Huang, H. Sun, Biochem. J. 393 (2006) 285-293.

[14] R. Ge, Y. Zhang, X. Sun, R.M. Watt, Q.Y. He, J.D. Huang, D.E. Wilcox, H. Sun, J. Am. Chem. Soc. 128 (2006) 11330-11331.

[15] S.L. Benoit, E.F. Miller, R.J. Maier, Infect. Immun. 81 (2013) 580-584.

[16] X. Sun, C.-N. Tsang, H. Sun, Metallomics 1 (2009) 25-31.

[17] H. Li, H. Sun, Curr. Opin. Chem. Biol. 16 (2012) 74-83.

[18] N. Yang, H. Sun, Coord. Chem. Rev. 251 (2007) 2354-2366.

[19] R. Ge, H. Sun, Acc. Chem. Res. 40 (2007) 267-274.

[20] W. Li, L. Jin, N. Zhu, X. Hou, F. Deng, H. Sun, J. Am. Chem. Soc. 125 (2003) 12408-12409.

[21] S.V. Wegner, E. Ertem, M. Sunbul, C. He, Chem. Sci. 2 (2011) 451-456.

[22] D.S. Folk, J.C. Torosian, S. Hwang, D.G. McCafferty, K.J. Franz, Angew. Chem. Int. Ed. 51 (2012) 10795-10799.

[23] H. Ma, E.A. Gibson, P.J. Dittmer, R. Jimenez, A.E. Palmer, J. Am. Chem. Soc. 134 (2012) 2488-2491.

[24] K.M. Dean, Y. Qin, A.E. Palmer, Biochim. Biophys. Acta Mol. Cell Res. 1823 (2012) 1406-1415.

[25] A.J. Lam, F. St-Pierre, Y. Gong, J.D. Marshall, P.J. Cranfill, M.A. Baird, M.R. McKeown, J. Wiedenmann, M.W. Davidson, M.J. Schnitzer, R.Y. Tsien, M.Z. Lin, Nat. Meth. 9 (2012) 1005-1012.

[26] S.V. Wegner, H. Arslan, M. Sunbul, J. Yin, C. He, J. Am. Chem. Soc. 132 (2010) 2567-2569.

[27] J.L. Vinkenborg, T.J. Nicolson, E.A. Bellomo, M.S. Koay, G.A. Rutter, M. Merkx, Nat. Meth. 6 (2009) 737-740.

[28] F.C. Neidhardt, P.L. Bloch, D.F. Smith, J. Bacteriol. 119 (1974) 736-747.

[29] A.M. Waterhouse, J.B. Procter, D.M.A. Martin, M.l. Clamp, G.J. Barton, Bioinformatics 25 (2009) 1189-1191.

[30] J.N. Weiss, FASEB J. 11 (1997) 835-841.

[31] H.L. Mobley, R.M. Garner, G.R. Chippendale, J.V. Gilbert, A.V. Kane, A.G. Plaut, Helicobacter 4 (1999) 162-169.

[32] L. Hu, T. Cheng, B. He, L. Li, Y. Wang, Y.-T. Lai, G. Jiang, H. Sun, Angew. Chem. Int. Ed. 52 (2013) 4916-4920.

[33] N.M. Chiera, M. Rowinska-Zyrek, R. Wieczorek, R. Guerrini, D. Witkowska, M. Remelli, H. Kozlowski, Metallomics 5 (2013) 214-221.

[34] D. Witkowska, S. Bielinska, W. Kamysz, H. Kozlowski, J. Inorg. Biochem. 105 (2011) 208-214.

[35] M. Vaara, Microbiol. Rev. 56 (1992) 395-411.

[36] T. Cheng, W. Xia, P. Wang, F. Huang, J. Wang, H. Sun, Metallomics 5 (2013) 1423-1429.

[37] M.D. Michelitsch, J.S. Weissman, Proc. Natl. Acad. Sci. USA 97 (2000) 11910-11915.

[38] F. Fiumara, L. Fioriti, E.R. Kandel, W.A. Hendrickson, Cell 143 (2010) 1121-1135.

[39] L. Guo, A. Han, D.L. Bates, J. Cao, L. Chen, Proc. Natl. Acad. Sci. USA 104 (2007) 4297-4302.

[40] D. Witkowska, M. Rowinska-Zyrek, G. Valensin, H. Kozlowski, Coord. Chem. Rev. 256 (2012) 133-148.

[41] P. Kalab, K. Weis, R. Heald, Science 295 (2002) 2452-2456.

[42] J. Brumbaugh, A. Schleifenbaum, A. Gasch, M. Sattler, C. Schultz, J. Am. Chem. Soc. 128 (2005) 24-25.

[43] S.M. Yannone, S. Hartung, A.L. Menon, M.W. Adams, J.A. Tainer, Curr. Opin. Biotechnol. 23 (2012) 89-95.